Enhancing the Mechanical and Fracture Properties of Nanocomposites Using Carbon Nanotubes

K.J. Loh[*,1], M. Thouless[2], J.P. Lynch[2]
[1]*University of California, Davis, California, USA;* [2]*University of Michigan, Ann Arbor, Michigan, USA*

1. Introduction

Recent technological advances in the nanotechnology field have permitted the design of polymeric thin films and polymer-based nanocomposites for energy storage [1], high-k dielectrics [2], light-emitting diodes [3], actuators [4], sensors [5], among many others. While these thin films have been tailored to exhibit unique optical, electrical, and electromechanical properties, enhancements in mechanical performance can improve their robustness and durability for use in complex and harsh operating environments. In fact, many researchers have sought to take advantage of the impressive properties (*i.e.*, strength and stiffness) of carbon nanotubes (CNT) [6] to enhance the mechanical attributes of these materials. A recent review conducted by Coleman, *et al.* [7] has summarized efforts to incorporate carbon nanotubes within composites fabricated via epoxy-setting, thermosets, melts, *in situ* polymerization, among many others. In general, the bulk composite stiffness, strength, and hardness have been found to increase in tandem with increasing carbon nanotube weight content [7].

In this study, single-walled carbon nanotubes (SWNT) are employed to mechanically reinforce layer-by-layer (LbL) self-assembled nanocomposites. Previous studies have already demonstrated that judicious selection of LbL polymeric constituents and the incorporation of SWNTs yield thin film strain and pH sensors [8]. By optimizing the weight content of nanotubes deposited during LbL, thin films can also be *tuned* to exhibit impressive mechanical performance. Thus, to explore the dependency of the bulk nanocomposite mechanical properties on SWNT weight content, SWNT solution concentrations used during LbL are varied between 0 to 0.5 mg-mL^{-1}. Post-fabrication treatment techniques such as thermal annealing are employed to cross-link polymer chains to further enhance the mechanical behavior of the thin films. Extensive experimental monotonic tensile tests are conducted for correlating SWNT content with bulk mechanical properties such as Young's modulus, ultimate tensile strength, and ultimate failure strain. Moreover, edge cracks are also introduced to thin film specimens for characterizing nanocomposite resistance to fracture failure (*i.e.*, for measuring nanocomposite fracture toughness and energy-release rate).

[*] Assistant Professor, Department of Civil & Environmental Engineering, University of California, One Shields Avenue, 3155 Engineering III, Davis, CA 95616, USA; TEL: +1 (530) 754-9428, E-mail: kjloh@ucdavis.edu.

Table 1. A list of nanocomposites fabricated for mechanical testing.

Thin Film Composition Name	SWNT Concentration	Polyanionic Solution	Polycationic Solution
Type A – Control	0	1.0 *wt.* % PSS	1.0 *wt.* % PVA
Type B – Low Concentration	0.25 mg-mL^{-1}	1.0 *wt.* % PSS	1.0 *wt.* % PVA
Type C – High Concentration	0.50 mg-mL^{-1}	1.0 *wt.* % PSS	1.0 *wt.* % PVA

2. Experimental Details

2.1. Layer-by-Layer Nanocomposite Fabrication and Thermal Treatment

Homogeneous SWNT-polyelectrolyte (PE) nanocomposites are fabricated via a systematic layer-by-layer self-assembly technique [9]. Layer-by-layer assembly entails the sequential dipping of a charged substrate (*e.g.*, glass, silicon, metals, among others) in oppositely-charged solutions to deposit various nanomaterials one monolayer at a time (Fig. 1). Selective deposition of each additional monolayer is based on opposite charge electrostatic and van der Waals force interaction with the preceding monolayer [9].

The first polyelectrolyte monolayer in the LbL assembly process is deposited by dipping a clean, charged glass microscope slide (treated with 3:7 H_2O_2:H_2SO_4 piranha solution) in a polycationic 1.0 *wt.* % poly(vinyl alcohol) (PVA, Sigma) aqueous solution for 5 min. Excessively large particulates and loosely-adsorbed PE species are rinsed off in 18 MΩ deionized water for 3 min, followed by a drying step for 10 min. Next, deposition of the SWNT-based monolayer is achieved by dipping the PE-coated substrate in a negatively-charged SWNT (Carbon Nanotechnologies, Inc.) suspension for 5 min, followed by the rinsing (3 min) and drying steps (10 min). Here, a 1.0 *wt.* % poly(sodium 4-styrene sulfonate) (PSS, $M_w \approx$ 1,000,000, Aldrich) solution is employed to achieve a stable SWNT dispersion of various concentrations (0, 0.25 and 0.50 mg-mL^{-1}) [8]. This process completes one full cycle of the LbL process to form one bilayer of the SWNT-PE nanocomposite. Multilayer thin film assembly is realized by repeating the aforementioned procedure to fabricate free-standing films of 200 bilayers, whereby these thin films will be referred to as (SWNT-PSS/PVA)$_{200}$.

In addition, enhancement of thin-film mechanical properties is conducted by thermally annealing each film in a furnace at 180 ºC for 20 min. Then, a 1.0 *vol.* % hydrofluoric acid bath is employed to chemically etch the glass to release free-standing (SWNT-PSS/PVA)$_{200}$ films. In total, three types of unique films will be mechanically tested to extract their mechanical and fracture properties (Table 1).

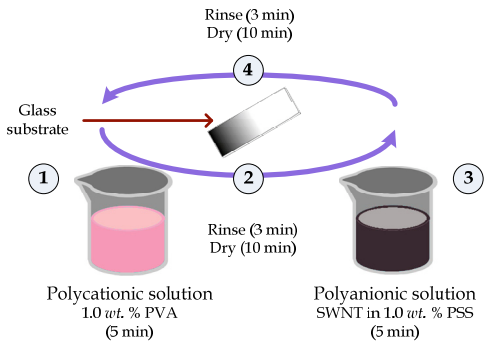

Figure 1. A schematic illustrating the layer-by-layer fabrication process.

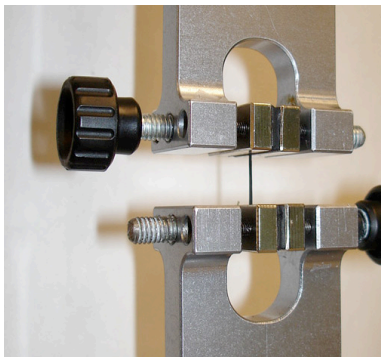

Figure 2. $(SWNT\text{-}PSS/PVA)_{200}$ thin film loaded in the Q100 load frame.

2.2. Mechanical Testing of Carbon Nanotube-Reinforced Thin Films

Experimental monotonic tensile testing of free-standing $(SWNT\text{-}PSS/PVA)_{200}$ thin films is required to determine the Young's modulus, ultimate tensile strength, and ultimate failure strain of these materials. Nanocomposite samples are cut into approximately 25 x 2 mm^2 specimens and loaded in a TestResources Q100 mechanical load frame (Fig. 2). Fixed-fixed boundary conditions are ensured, and the final unsupported length of the loaded specimens is approximately 12 mm. It should be noted that precise thin film dimensions (length and width) are measured using a digital caliper with ±0.005 mm resolution. The scanning electron microscope (SEM) is used to determine average thin film cross-sectional thickness (where $h \approx 1$ μm for most specimens tested).

Upon sample loading, the TestResources Q100 load frame is commanded to execute a uniaxial and monotonic tensile load pattern at a displacement-controlled 10 μm-s^{-1} load rate while the embedded data acquisition system (DAQ) samples time, stroke displacement, and equilibrium load simultaneously at 15 Hz. It should be mentioned that stroke displacement of the Q100 load frame is used to calculate induced strains due to the inherent difficulty of physically attaching an extensometer onto thin films characterized by micro-meter thicknesses.

2.3. Nanocomposite Fracture Toughness Measurements

The fracture toughness and critical stress-intensity factors of the nanocomposites are determined by employing a similar experimental procedure described in Section 2.2. In this case, thin films are cut into approximately 25 x 4 mm^2 to 25 x 6 mm^2 samples to preserve the specimen's high aspect ratio while simultaneously producing a wide specimen width for introducing an initial edge crack (of length a_0) 0.5 to 1.0 mm long that is perpendicular to one side and near the midsection of

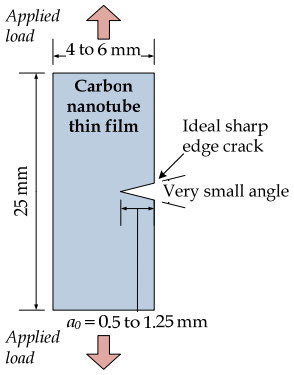

Figure 3. The experimental setup employed to measure nanocomposite fracture toughness.

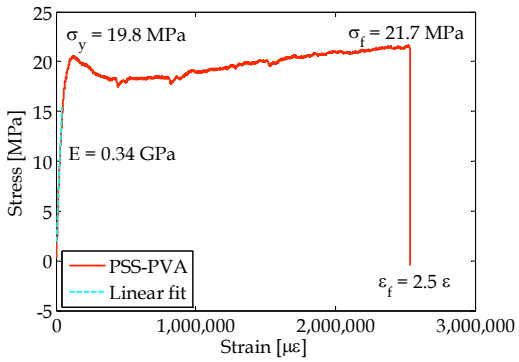

Figure 4. The typical stress-strain response of pure polymeric PSS-PVA thin films (Type A specimen).

each specimen (via mechanical cutting with a razor blade). Then, the edge-cracked film is loaded in the TestResources Q100 load frame using the same load pattern and load rate described in Section 2.2 (Fig. 3). The DAQ is commanded to record time, applied load, and stroke displacement at 15 Hz as before. In addition, a JVC GZ-MG255U digital video camera is employed to optically image thin films at 30 fps (frames per second) during loading to monitor crack propagation.

3. Experimental Results and Discussion

3.1. Enhancement of Nanocomposite Mechanical Properties

In order to obtain the baseline mechanical properties of the aforementioned films, specimens of Type A of Table (1) (*i.e.*, no SWNT reinforcement) are mechanically tested to characterize its stress-strain response to monotonic tensile loading, and the stress-strain response is shown in Fig. (4). It can be seen that PSS-PVA thin films exhibit a stress-strain response typical of polymeric materials. Upon initial loading, Type A specimens exhibit excellent linearity up to 100,000 με (10% strain), followed by initial yielding, then significant plasticity observed from homogeneous crazing across the entire length of the specimen (Fig. 4). It should be noted that crazing initiates after the applied strain exceeds 1 ε or 100% strain. In this case, strain hardening behavior is due to interlocking of physical entanglements within the PSS and PVA polymer chains. Linear regression of the initial stress-strain curve suggests that the average Young's modulus (E) of PSS-PVA films is approximately 0.33 ± 0.01 GPa. Likewise, the ultimate strength (σ_f) and ultimate strain (ε_f) is 20.7 ± 0.8 MPa and 2.53 ± 0.16 ε (253% strain), respectively. Thus, it can be concluded that PSS-PVA thin films exhibit high ductility, moderate ultimate strength, but very low stiffness.

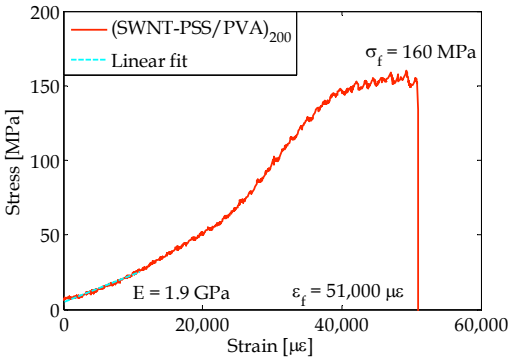

Figure 5. The typical stress-strain response of $(SWNT\text{-}PSS/PVA)_{200}$ thin films fabricated from 0.25 mg-mL^{-1} SWNT-PSS solutions (Type B).

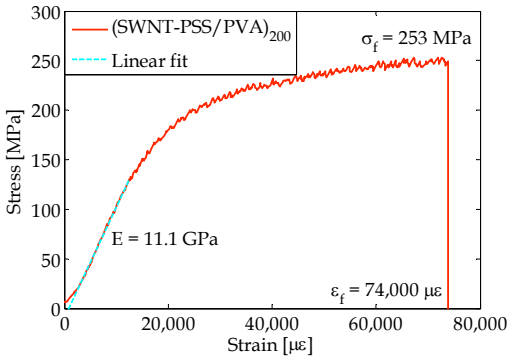

Figure 6. The typical stress-strain response of $(SWNT\text{-}PSS/PVA)_{200}$ thin films fabricated from 0.50 mg-mL^{-1} SWNT-PSS solutions (Type C).

Using the same procedure outlined in Section (2.2), Types B and C films of Table (1) have also been mechanically tested for obtaining their stress-strain response. For nanocomposites fabricated with 0.25 mg-mL^{-1} SWNT-PSS solutions (*i.e.*, Type B films), the average Young's modulus, ultimate strength, and ultimate strain are 1.9 ± 0.1 GPa, 157 ± 9 MPa, and 48,700 ± 1,000 με, respectively. For Type C films, E = 11.2 ± 0.4 GPa, σ_f = 229 ± 7 MPa, and ε_f = 67,000 ± 3,900 με. Representative stress-strain curves for films of Types B and C are presented in Fig. (5) and Fig. (6), respectively, and a summary of thin film mechanical properties for the different types of films are shown in Table (2).

First, dramatic improvements in thin film mechanical properties are achieved by thermal annealing of these carbon nanotube-based composites. As compared to a previous study conducted by Loh, *et al.* [10], as-fabricated (*i.e.*, non-annealed) $(SWNT\text{-}PSS/PVA)_{200}$ thin films' stress-strain response is initially linear (up to 10,000 με) followed by sudden brittle failure at ε_f = 21,000 με (only mild yielding and no strain hardening has been observed). On average, film stiffness is 8.5 GPa, and the ultimate tensile strength is 128 MPa. In general, a two-fold enhancement of stiffness, ultimate strength, and ultimate strain are obtained in this study simply by polymer cross-linking and thermal treatment of LbL nanocomposites.

Second, it is apparent from Table (2) that enhanced strength and stiffness are also attained when initial SWNT-PSS solution concentrations are increased from 0 to 0.5 mg-mL^{-1}. In fact, for both the nanocomposite's bulk Young's modulus and ultimate tensile strength, an order of magnitude increase in mechanical properties can be obtained as shown in Table (2). Among all of the films tested, all specimens displayed linearity upon initial loading (to more than 10,000 με). Beyond 10,000 με, yielding occurs, followed by moderate strain hardening for Type B films (low nanotube concentration) and enhanced strain hardening for Type C films. Thus, results from this study permit the tailoring of thin film mechanical properties characterized by unique stress-strain relationships.

Table 2. Summary of mechanical properties of thin film fabricated from different SWNT-PSS solution concentrations.

SWNT weight content	0 mg-mL^{-1}	0.25 mg-mL^{-1}	0.50 mg-mL^{-1}
Young's Modulus	0.33 GPa	1.9 GPa	11.2 GPa
Ultimate Strength	21 MPa	157 MPa	229 MPa

3.2. Thin Film Fracture Toughness

When measuring the fracture toughness of homogeneous isotropic materials, it is important to determine whether materials undergo plane strain or plane stress. Given a bulk material subjected to uniaxial tensile loading, a large localized stress region develops near the vicinity of a crack tip. At this localized stress region, a plastic zone is created, and the material near the crack tip is at its yield stress. At such high localized stresses and strains, the inherent material response is to contract laterally due to Poisson's effect. However, such contractions are prevented if a thick material is being tested, thereby undergoing plane strain. In the case of thin film materials, the size of the developed plastic zone is often comparable to the specimen thickness; consequently, the film is free to contract to relieve stresses in the direction of film thickness so that they undergo plane stress [11, 12].

The stress-intensity factor (K_I) is the loading parameter used to describe the crack-driving force. For the geometry shown in Fig. (3), which is only mode-I, the crack is normal to the applied load, and the stress-intensity factor is calculated by [11]:

$$K_I = f(a/W)\sigma\sqrt{a} \tag{1}$$

where σ is the remote stress, a is the crack length, W is the film's width, and $f(a/W)$ is a geometric correction factor. In general, crack propagation is assumed to occur when the stress-intensity factor is equal to the material's fracture toughness (K_{Ic}). However, in a material that exhibits R-curve behavior (fracture toughness increasing with crack extension), there are several different measures for the onset of cracking. The initiation fracture toughness, K_{Ii}, corresponds to the stress-intensity factor for the initial crack to start growing, while the fracture toughness corresponds to the stress-intensity factor at which a growing crack reaches an instability condition. In this study, we measure an effective fracture toughness determined from the initial crack length (a_0) measured before the experiment and the maximum stress (σ_f) corresponding to the point of instability:

$$K_{Ie} = f(a/W)\sigma_f\sqrt{a_0} \tag{2}$$

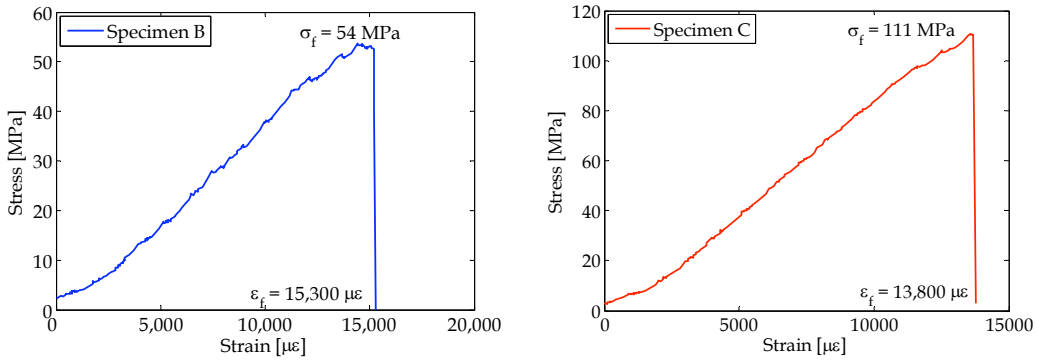

(a) (b)

Figure 7. Stress-strain responses of $(SWNT\text{-}PSS/PVA)_{200}$ thin films with an initial edge crack of size a_0 and fabricated with (a) 0.25 mg-mL^{-1} (Type B) and (b) 0.50 mg-mL^{-1} (Type C) SWNT-PSS solutions.

3.3. Determining LbL Nanocomposite Fracture Toughness

Fig. (7) plots the typical stress-strain responses for post-annealed $(SWNT\text{-}PSS/PVA)_{200}$ thin films fabricated with different initial SWNT concentrations. These films have been mechanically cut with an initial edge crack of length a_0 (0.5 to 1.25 mm), and subjected to uniaxial monotonic tensile loading. Comparing Fig. (7) to the previous stress-strain curves shown in Fig. (5) and Fig. (6), it can be clearly seen that these edge-cut nanocomposites fail at much lower ultimate stresses and strains. As opposed to yielding and strain hardening (Fig. 5 and Fig. 6), these specimens fail by sudden fracture initiating from the initial edge crack.

To determine the effective fracture toughness of LbL $(SWNT\text{-}PSS/PVA)_{200}$ nanocomposites, Eq. (2) is employed. For the nanocomposite specimens that have been fracture-tested, the geometric correction factor is given by Anderson [11] as:

$$f(a/W) \approx 1.12 \tag{3}$$

Thus, using Eq. (3), the mode-I effective stress-intensity factor is expressed in Eq. (4) as [11]:

$$K_{Ie} = 1.12\sigma_i\sqrt{a_0} \tag{4}$$

For the thin films investigated in this study (Table 1), the average mode-I initiation fracture toughness is approximately 0.52, 1.55 ± 0.20, and 2.51 ± 0.12 MPa-√m for thin film Types A, B, and C (Table 1), respectively. It should be mentioned that the use of linear-elastic fracture mechanics is valid because the stress-strain curves for the test geometry are essentially linear up to the point of fracture. From the summary of nanocomposite fracture properties shown in Table

Table 3. Summary of fracture properties of thin film fabricated from different SWNT-PSS solution concentrations.

SWNT weight content	**0 mg-mL^{-1}**	**0.25 mg-mL^{-1}**	**0.50 mg-mL^{-1}**
Fracture Toughness, K_{Ie}	0.52 MPa-√m	1.55 MPa-√m	2.51 MPa-√m
Toughness, Γ	141 J-m^{-2}	15.2 J-m^{-2}	27.5 J-m^{-2}

(3), it is obvious that fracture toughness increases near-linearly with increasing carbon nanotube content.

These fracture tests indicate that the fracture toughness increases with nanotube content; however, while the fracture toughness gives a measure of the strength of a cracked material, it is a combination of two distinct fundamental material properties, namely the elastic modulus (E) and the toughness (or critical energy-release rate). This latter quantity (Γ) is a measure of the energy dissipated in creating a unit area of new crack surface. Under plane-stress conditions, the fracture toughness is given by:

$$K_{Ic} = \sqrt{E\Gamma} \tag{5}$$

It is of fundamental interest to determine whether the rise in fracture toughness noted above arises from an increase in energy dissipation from the interaction of the crack tip with the nanotubes or merely due to an increase in the modulus. Using the values of modulus given in Table (2) and Eq. (5), it can be seen from Table (3) that the critical mode-I energy release rate is 141, 15.2, and 27.5 J-m^{-2} for nanocomposite Types A, B, and C, respectively. As seen from Table (3), the addition of nanotubes to form SWNT-reinforced nanocomposites significantly degrades the toughness of PSS/PVA thin films. This is probably caused by the constraint on crack-tip yielding introduced by the nanotubes; the reduced yielding results in a reduced level of energy dissipation during crack propagation. The rise in fracture toughness (and hence strength) of the nanocomposite arises only because of the dramatic increase in the stiffness (E). While high values of fracture toughness (K_{Ic}) enhance the strength of a material, the low value of toughness (Γ) makes the material more sensitive to flaws and liable to brittle failure. Thus, a tradeoff exists between increasing nanocomposite's strength and stiffness versus its resistance to brittle failure.

4. Conclusions

In summary, the main objective of this study is to provide mechanical reinforcement (*i.e.*, in the form of strength, stiffness, and toughness) to nanocomposites by embedding SWNTs within bulk LbL polymeric matrices. Experimental monotonic tensile testing of pure PSS-PVA thin films and $(SWNT\text{-}PSS/PVA)_{200}$ thin films fabricated with 0.25 and 0.50 mg-mL^{-1} SWNT-PSS concentrations reveal significant enhancements in the films' mechanical properties. Specifically, nanocomposites reinforced with 0.50 mg-mL^{-1} SWNTs exhibit an average stiffness, ultimate tensile strength, and ultimate failure strain of 11.2 ± 0.4 GPa, 229 ± 7 MPa, and 67,000 ± 3,900 με, respectively. Stress-strain curves obtained also demonstrate significant strain hardening after yielding.

The nanocomposites' fracture properties are also investigated via tensile testing of edge-cracked specimens. It has been shown that these thin films exhibit improvements in fracture toughness with increasing nanotube weight content. Despite fracture toughness improvements, the inclusion of nanotubes causes the nanocomposite to become more brittle as has been revealed by calculations of the critical energy-release rates. Having characterized the mechanical performance of these nanocomposites to mechanical loading, one can leverage the advantages of enhancing strength and stiffness with the material's inherent brittleness by controlling nanotube composition within the bulk polymeric matrix.

5. Acknowledgements

The authors would like to express their sincere gratitude to the National Science Foundation (NSF) Grant No. CMMI-0528867 (under program manager: Dr. S.C. Liu) for support of this research. In addition, the authors would also like to thank Professor Nicholas Kotov and his research group for providing access to the TestResources Q100 load frame.

6. References

[1] Li, Z.H., Zhang, H.P., Zhang, P., Wu, Y.P. and Zhou, X.D., Macroporous Nanocomposite Polymer Electrolyte for Lithium-Ion Batteries, Journal of Power Sources 184 (2) (2008) 562-565.

[2] Lu, J., Moon, K.-S. and Wong, C.P., Silver/Polymer Nanocomposite as High-K Polymer Matrix for Dielectric Composites with Improved Dielectric Performance, Journal of Materials Chemistry 18 (40) (2008) 4821-4826.

[3] Park, O.O., Park, J.H., Kim, T.-H., Yu, J.-W., Kim, J.K. and Kim, Y.C., Enhanced Color Purity and Stability from Polymer/Nanoporous Silica Nanocomposite Blue Light-Emitting Diodes, Synthetic Metals 154 (1-3) (2005) 145-148.

[4] Jung, J.-Y. and Oh, I.-K., Novel Nanocomposite Actuator Based on Sulfonated Poly(Styrene-B-Ethylene-Co-Butylene-B-Styrene) Polymer, Journal of Nanoscience and Nanotechnology 7 (11) (2007) 3740-3743.

[5] Jiang, C., Markutsya, S., Pikus, Y. and Tsukruk, V.V., Freely Suspended Nanocomposite Membranes as Highly Sensitive Sensors, Nature Materials 3 (10) (2004) 721-728.

[6] Iijima, S., Helical Microtubules of Graphitic Carbon, Nature 354 (6348) (1991) 56-58.

[7] Coleman, J.N., Khan, U. and Gun'ko, Y.K., Mechanical Reinforcement of Polymers Using Carbon Nanotubes, Advanced Materials 18 (6) (2006) 689-706.

[8] Loh, K.J., Kim, J., Lynch, J.P., Kam, N.W.S. and Kotov, N.A., Multifunctional Layer-by-Layer Carbon Nanotube-Polyelectrolyte Thin Films for Strain and Corrosion Sensing, Smart Materials and Structures 16 (2) (2007) 429-438.

[9] Decher, G. and Schlenoff, J.B., ed., Multilayer Thin Films: Sequential Assembly of Nanocomposite Materials, Wiley-VCH, Federal Republic of Germany, 2003.

[10] Loh, K.J., Development of Multifunctional Carbon Nanotube Nanocomposite Sensors for Structural Health Monitoring, Ph.D. Thesis, University of Michigan, Department of Civil & Environmental Engineering, Ann Arbor, MI, 2008.

[11] Anderson, T.L., Fracture Mechanics: Fundamentals and Applications, CRC Press, Boca Raton, FL, 1995.

[12] Klemann, B.M. and Devilbiss, T., The Fracture Toughness of Thin Polymeric Films, Polymer Engineering and Science 36 (1) (1996) 126-134.

[13] Irwin, G.R., Onset of Fast Crack Propagation in High Strength Steel and Aluminum Alloys, Proceedings of Sagamore Research Conference 2 (1956) 289-305.